Exogenous Retinoic Acid During Gastrulation Induces Cartilaginous and Other Craniofacial Defects in *Fundulus heteroclitus*

MARK W. VANDERSEA[1], ROBERT A. McCARTHY[1,2], PAUL FLEMING[1,2], AND DENICE SMITH[1,*]

[1] *Grice Marine Biological Laboratory, University of Charleston, 205 Fort Johnson, Charleston, South Carolina 29412; and* [2] *Department of Cell Biology and Anatomy, Medical University of South Carolina, Charleston, South Carolina 29401*

Abstract. Embryonic levels of retinoic acid (RA) and the response of cells to RA are critical to the normal development of vertebrates. To understand the effects of RA signaling in *Fundulus heteroclitus*, we exposed embryos to a range of RA concentrations for 2 h during gastrulation. Embryos exposed to low concentrations of RA (10^{-10}–10^{-7} M) develop normally, whereas those exposed to higher concentrations (5×10^{-7}–10^{-4} M) develop characteristic dose-dependent defects. We describe, in detail, four stages of development that represent morphological effects of RA on (1) cell death and defects in the brain, heart, and eye, (2) relative size and differentiation, (3) duplications of pectoral fins, and (4) deletions in craniofacial cartilage elements. Analysis of cartilaginous skeletal elements demonstrates distinct patterns of deletions in the neurocranium and pharyngeal skeleton in response to increasing concentrations of RA. In *F. heteroclitus*, RA treatment during gastrulation results in five highly consistent phenotypes, which we have incorporated into an index of embryonic RA defects. This index should be valuable in the genetic analysis of RA pathways and in evaluating chemicals that interfere with embryonic RA signaling.

Introduction

Retinoic acid (RA), a derivative of vitamin A, is reported to be an important signaling molecule that plays a crucial role in establishing anterior-posterior patterning in vertebrate embryos (for review see Means and Gudas, 1995). Endogenous RA has been detected in many vertebrate organisms (Durston *et al.*, 1989; Chen *et al.*, 1992; Hogan *et al.*, 1992) including *Xenopus laevis*, in which developing embryos exhibit a gradient of RA (Chen *et al.*, 1994). RA binds to receptors that are members of a large superfamily of steroid and thyroid hormone binding receptors (Lohnes *et al.*, 1995). RA and the receptors then recognize DNA response elements that influence gene expression by promoting or inhibiting transcription (Marshall *et al.*, 1994; Zilliacus *et al.*, 1995). Developmental target genes include Hox genes (Langston and Gudas, 1992; Studer *et al.*, 1994; Lohnes *et al.*, 1995), which impart important anterior-posterior positional information along the axis of the developing embryo (Kessel and Gruss, 1991; Kessel, 1992; and Krumlauf, 1994).

The distribution of RA in the embryo is heterogeneous and the concentration is both limiting and critical because patterning defects can be induced by both RA excess (Holder and Hill, 1991) and RA deficiency (Schuh *et al.*, 1993). Embryos respond to RA in a dose-dependent and stage-specific manner (Durston *et al.*, 1989; Sive *et al.*, 1990; Holder and Hill, 1991; Wood *et al.*, 1994). The sensitivity of vertebrate embryos to RA is well documented in mouse (Wood *et al.*, 1994; Leonard *et al.*, 1995), *Xenopus* (Durston *et al.*, 1989; Minucci *et al.*, 1996; Sive *et al.*, 1990), chicken (Gale *et al.*, 1996), and zebrafish (Holder and Hill, 1991; Stainier and Fishman, 1992; Hill *et al.*, 1995). Exposure of zebrafish embryos to RA during gastrulation results in deletions of the midbrain-hindbrain border regions; defects in the eye, retina,

and heart; deformities of the tail; and abnormalities in the cartilaginous skeletal elements of the head (Holder and Hill, 1991; Stainier and Fishman, 1992; Alexandre *et al.*, 1996). Administered later in development, exogenous RA can disrupt the patterning of the fin (Akimenko and Ekker, 1995). In chicken and quail embryos, application of RA to the anterior of a limb bud often results in a mirror-image duplication of digits (Tickle, 1995; Tabin, 1995). This suggests that a delicate balance of RA is critical to the proper patterning of embryonic structures and that disruption of this signaling pathway results in a variety of skeletal and anatomical malformations.

In vertebrates, much of the head skeleton is derived from neural crest precursors that migrate into the pharyngeal arches from the midbrain and specific rhombomeres of the hindbrain (Langille and Hall, 1988, 1993). Specific populations of neural crest cells that contribute to the skeletal elements in the head have been identified in mapping studies (Couly *et al.*, 1993; Schilling and Kimmel, 1994). Among different vertebrates, the similarities of neural crest contributions to skeletal elements suggests that the patterning mechanisms that direct these cells are also well conserved (Koentges and Lumsden, 1996; Schilling and Kimmel, 1994; Noden, 1975). The molecular mechanism by which the craniofacial skeleton is patterned is not fully understood. However, interactions between rhombomeric segments of the hindbrain, neural crest cells, and branchial arches are thought to be influenced by overlapping expression domains of Hox genes; moreover, the anterior-posterior patterning of the head is regulated by a Hox code in the branchial region (Hunt *et al.*, 1991) that may be influenced by endogenous RA.

In this study we exposed *F. heteroclitus* embryos to a range of RA concentrations during gastrulation, and we describe defects in the treated embryos as they appear at four distinct developmental stages. In other species, a large variation of phenotypes is produced in response to a single RA concentration (Holder and Hill, 1991; Marshall *et al.*, 1992), but the protracted development of *F. heteroclitus* has allowed for the selection of highly synchronous embryos that respond more uniformly. We show that disruption of endogenous levels of RA during gastrulation results in deletions of the midbrain-hindbrain border region and, at higher concentrations, to deletion of the eyes, shortening of the trunk, and duplications of the pectoral fins. Analysis of cartilage in these embryos suggests that RA differentially affects the patterning of subpopulations of neural crest cells and the formation of specific cartilage elements, resulting in very different patterns of deletions in the neurocranium and the pharyngeal skeleton.

Bent body axes, fin defects, heart defects, eye malformations, and craniofacial defects are common in fish embryos that have been exposed to heavy metals and other xenobiotics during gastrulation (Weis and Weis, 1977; Sharp and Neff, 1980, 1985; Weis and Weis, 1989). These defects are similar to those induced by RA excess or deficiency, suggesting that xenobiotics may interfere with embryonic RA signaling pathways. Therefore, one objective of this study was to utilize *F. heteroclitus*—an estuarine species widely used in toxicity studies—as a model with which to establish an index of defects that occur in response to disruption of RA signaling. The index we describe should therefore help identify and evaluate the sensitivity of embryos to the effects of xenobiotics on RA-regulated pathways.

Materials and Methods

In vitro fertilization of F. heteroclitus

Adult fish were captured from a *Spartina* marsh adjacent to the Grice Marine Biological Laboratory, Charleston, South Carolina. Fish were anesthetized with $1.5 \times 10^{-4} M$ 3-aminobenzoic acid ethyl ester (MS-222) in filtered seawater. Eggs were collected from gravid females, in a dry dish, and then fertilized with 15 μl of sperm activated in 20 ml of filtered seawater. Eggs were then rinsed (15 min post-fertilization) and incubated in a moist chamber at 25°C. Only embryos that showed normal cell cleavage were used experimentally. At 10 days post-fertilization, the eggs were immersed in filtered seawater, which initiated hatching.

Staging series of F. heteroclitus

Embryos from *in vitro* fertilizations (about 100–300 eggs/fertilization) were raised at 25°C, a temperature relevant to the warm coastal waters of South Carolina. Their development was recorded and characterized from before fertilization until 2 days after hatching (12 days post-fertilization). Observations of anatomical features at different stages were compared with descriptions produced by Armstrong and Child (1965), Oppenheimer (1937), and Solberg (1938), and a staging series at 25°C was constructed.

Retinoic acid treatment

Stock solutions of $2 \times 10^{-2} M$ were made in dimethyl sulfoxide (DMSO) from all-*trans*-retinoic acid (Sigma Chemical Co.) and stored at −20°C. Experimental concentrations were prepared by serial dilution with filtered seawater (FSW). Embryos at 50% epiboly (from *in vitro* fertilizations; stage 17, 21.5 h post-fertilization (hpf) at 25°C) were exposed to concentrations of RA ranging from $10^{-10} M$ to $10^{-4} M$ for 2 h in the dark. DMSO control embryos were exposed to 0.1% DMSO in FSW, and untreated control embryos were incubated in FSW. All embryos were then rinsed for 10 min several times with large

Table 1

Comparison of embryonic development at 20°C[1] and 25°C

Stage	Time (h:min) 20°C	Time (h:min) 25°C	Stage	Time (h:min) 20°C	Time (h:min) 25°C
1	0	0	21	52:00	32:00
2	1:75	1:00	22	56:00	34:30
3	2:50	2:00	23	66:00	40:00
4	3:25	2:45	24	74:00	45:00
5	4:25	3:10	→25	84:00	51:00
6	5:00	3:40	26	92:00	63:00
7	6:00	4:30	27	112	73:00
8	7:50	6:00	28	128	82:30
9	9:00	7:00	→29	144	90:00
10	10:00	8:45	30	156	99:00
11	11:00	9:45	31	168	120
12	15:00	11:15	32	192	142
13	20:00	12:00	33	216	166
14	24:00	14:00	34	228	188
15	27:00	16:00	35	252	205
16	30:00	19:00	36	288	220
→17	33:00	21:30	→37	336	245
18	37:00	24:30	38	360	270
19	40:00	27:30	→39	384	296
20	46:00	30:00			

[1] Data from Armstrong and Child, 1965.
Arrows indicate stages and times relevant to this study.

volumes of FSW and allowed to develop at 25°C in a moist chamber.

Skeletal preparations of embryos, and photography

Skeletal preparations of stage 39 larvae were prepared by the method of Dingerkus and Uhler (1977), except that a 0.05% solution of trypsin in saturated sodium borate was used to digest the embryonic tissues. Camera lucida drawings of whole-mounted larvae stained with alcian blue were prepared with the aid of a drawing tube attached to a Nikon Optiphot 2 microscope. Drawings of live larvae were used to depict differences in size, overall morphology, and extent of development, and to serve as illustrations for the different levels of the RA index. Other images were obtained photographically with a Nikon SMZ-U dissecting microscope and Kodak film, digitized, and compiled with Adobe Photoshop software.

Results

During early development the embryo changes rapidly; thus, comparisons of the effects of RA on development demand precise staging and rearing of embryos. The developmental stages of *F. heteroclitus* raised at 20°C have been previously described by Armstrong and Child (1965). In our study, embryos were staged and raised at 25°C, reducing the time to hatching by about 4 days. Table I compares the development at 20°C to development

at 25°C, based on the staging descriptions of Armstrong and Child. To determine the effects of exogenous RA on *F. heteroclitus* at 50% epiboly (stage 17, Table 1), embryos were exposed for 2 h to concentrations of RA ranging from 10^{-10} M to 10^{-4} M and then allowed to develop at 25°C. Such embryos undergo gastrulation in the same manner as control embryos, and there are no immediate signs of cell death or toxic response. The overall axial dimensions of treated and control embryos are similar until stage 25, some 27 h after RA exposure, when embryos show normal trunk muscle development and slow muscle contractions.

We compared the development of RA-treated embryos and untreated embryos at four embryonic stages. At stage 25 (about 50 hpf; Table I), when an embryonic axis is completed, circulation begins, and head structures including the eyes and optic tecta are well formed. The overall dimensions of treated and untreated embryos are similar, but there are discernible differences in axial patterning. By stage 29 (about 90 hpf; Table I), dose-dependent effects of RA exposure are more pronounced, both in the relative size of the embryo and in organ differentiation. At stage 37 (about 245 hpf), untreated embryos and those exposed to 10^{-10}–10^{-7} M RA hatch, allowing observation of swimming movements and fin structure and comparisons of external morphology. Finally, at stage 39 (296 hpf), the cranial cartilage is well established and can be stained with alcian blue.

Stage 25: Early effects on eye, heart, and the midbrain-hindbrain region

1 × 10⁻⁶ M RA. At stage 25 (Fig. 1A) control embryos possess several anatomical landmarks useful for assessing the effects of RA. A small telencephalic ventricle (tv) is present in the forebrain. Embryos have well-defined eyes (arrows), optic tecta (ot), and a hindbrain (hb). Blood cells circulate in vessels on the yolk sac, and the heart is a broad tube with no defined chambers (not shown). Embryos exposed to low concentrations of RA (10^{-10} to 10^{-7} M) appear normal (compare Fig. 1A–E). In embryos treated with 10^{-6} M RA (Fig. 1F), the telencephalon (t) is present, although the telencephalic ventricle has not expanded (compare Fig. 1E and F), and the embryos display a slight anterior and ventral rotation of the eyes with the lenses incompletely filling the optic cups (arrows, Fig. 1F). Embryos exposed to this concentration lack well-defined optic tecta (asterisk, Fig. 1F). Moreover, most of the midbrain region appears deleted, and the hindbrain (hb) appears to have shifted slightly anteriorly (compare Fig. 1A and F). Using darkfield microscopy, cell death is apparent as white-opaque cells (Grunwald *et al.*, 1988; Stainier and Fishman, 1992) in the midbrain-hindbrain border region and along the trunk and tail (black arrow-
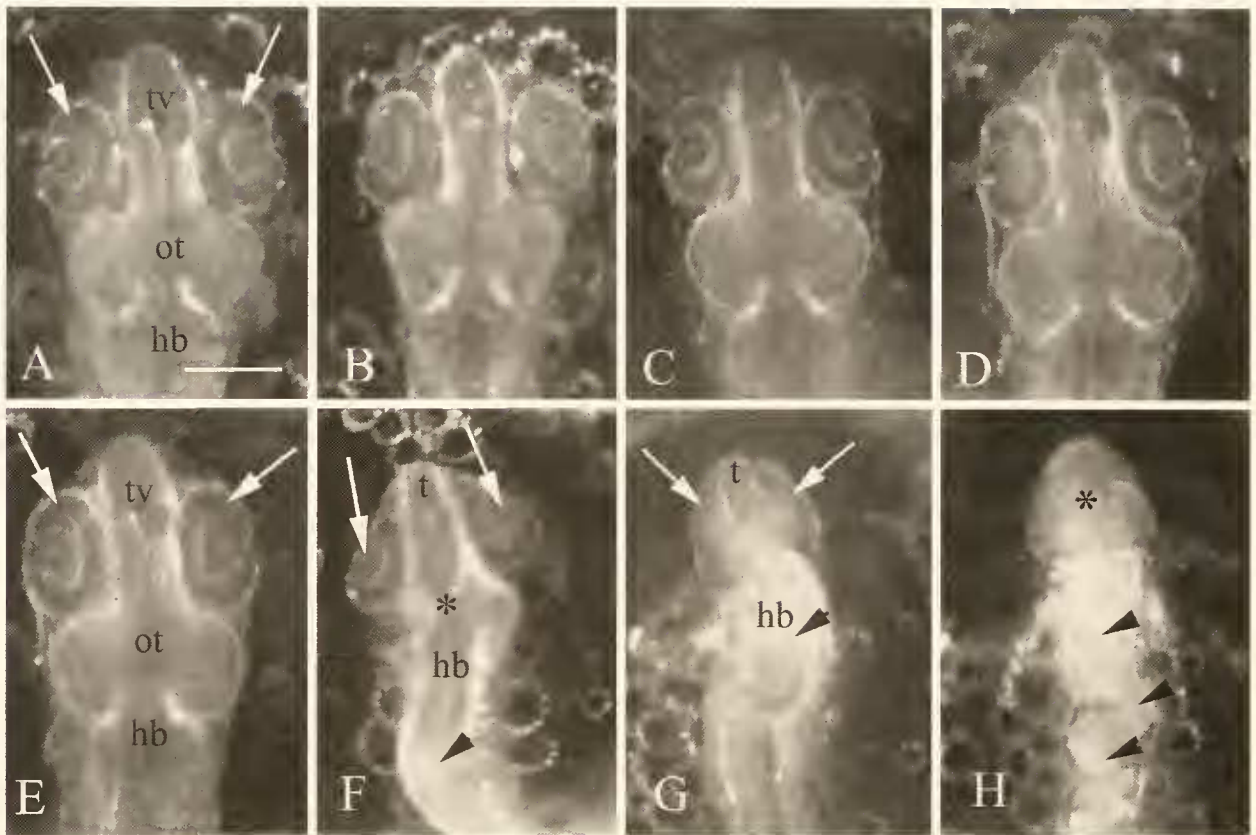
Figure 1. At stage 25, embryos exposed to retinoic acid (RA) during gastrulation show defects in the development of head structures. Control embryos (A) and embryos treated with low concentrations of RA—$10^{-10} M$ (B), $10^{-9} M$ (C), $10^{-8} M$ (D), and $10^{-7} M$ (E)—form an expanded telencephalic ventricle (tv, A and E) in the forebrain, optic tecta (ot) in the midbrain, and a well-developed hindbrain (hb). Embryos treated at gastrulation with $10^{-6} M$ RA (F) show defects in the eyes (arrows), telencephalon (t), and midbrain (asterisk). At $10^{-5} M$ (G), the telencephalon (t) and the eyes (arrows) are obscure. Note that the position of the hindbrain (hb, E, F, and G) assumes a progressively more anterior position. Cell death is indicated by black arrowheads (F, G, and H). Anterior is to the top. Scale bar = 200 μm.

head, Fig. 1F). Although not shown in Figure 1F, heart defects range from complete deletion of the heart to the development of a small, thin, tube heart. In those treated embryos that have a heart, circulation is not observed, even though cardiac contractions occur. Pericardial edema extends anteriorly over a large portion of the yolk, and blood cells pool in islands at the tip of the tail. The overall embryonic axis is slightly truncated, but muscular movements occur, and tails are often curled at the tips and are partially detached from the yolk.

1 × 10^{-5} M RA. Embryos exposed to 10^{-5} M RA show additional anterior head defects (Fig. 1G). Portions of the forebrain region and telencephalon (t) are present, but no telencephalic ventricle forms. The optic cups are ambiguous (arrows), and the midbrain-hindbrain border region is absent. The hindbrain (hb) lies immediately posterior to the forebrain region, and cell death is evident in the hindbrain region and along a posterior region of the trunk

(black arrowhead). Large pericardial edemas occur; the heart is deleted; and blood cells pool at the tip of the tail, which is still attached to the yolk (not shown). Although the embryo is truncated, muscular contractions occur.

1 × 10^{-4} M RA. Embryos exposed to 10^{-4} M RA show few forebrain and eye structures (asterisk, Fig. 1H). The embryonic axis is twisted and exhibits extensive degenerating white-opaque cells (black arrowheads). Muscular contractions of the trunk do not occur in the embryos at this stage. The heart is absent, but there is a large pericardial cavity, and blood cells are pooled posteriorly at the base of the tail.

Stage 29: Effects on relative size and differentiation

1 × 10^{-6} M RA. At stage 29 (Fig. 2) the embryonic head in control embryos has grown considerably; measurements of the area of the head indicate an enlargement
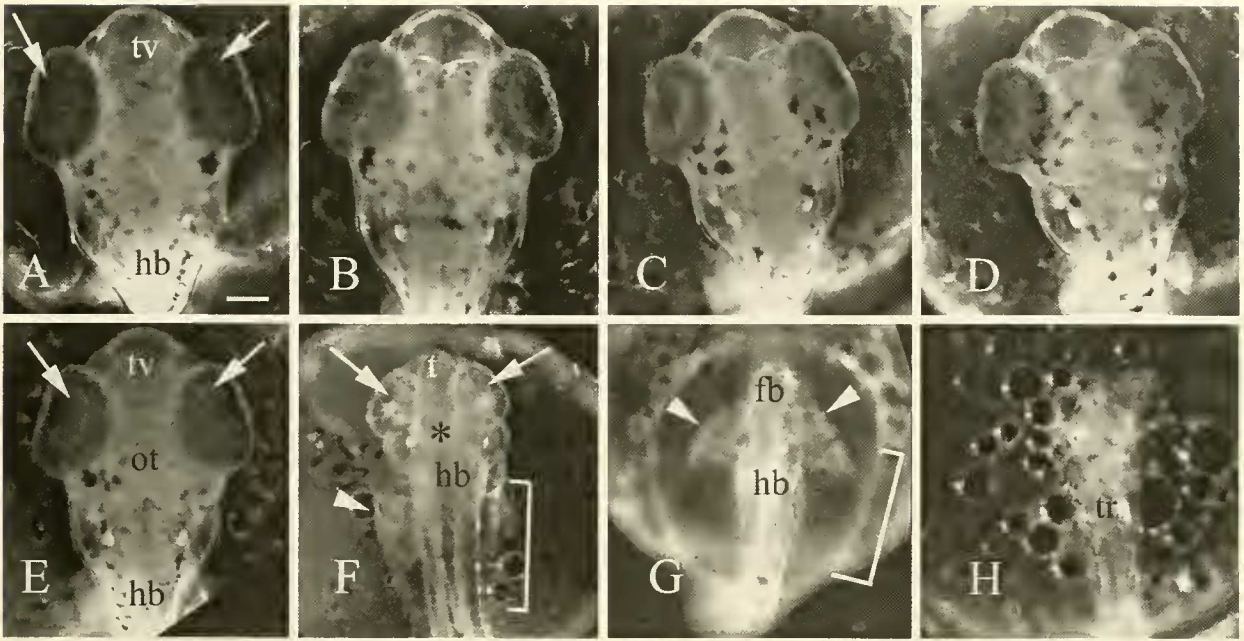
Figure 2. Dorsal views of stage 29 embryos show the effects of retinoic acid (RA) on relative size and head development. In control embryos (A) and embryos exposed to low concentrations of RA—$10^{-10}\,M$ (B), $10^{-9}\,M$ (C), $10^{-8}\,M$ (D), and $10^{-7}\,M$ (E), the eyes are lightly pigmented (arrows, A and E) and the telencephalic ventricle (tv, A and E) and optic tecta (ot, E) anterior to the hindbrain (hb, A and E) has expanded. Embryos exposed to $10^{-6}\,M$ RA lack retinal pigment in the eyes (arrows, F), show abnormalities of the brain (asterisk, F) anterior to the hindbrain (hb, F), pectoral fin development (arrowhead, F), and an expansion of the visceral cavity (bracket, F). At $10^{-5}\,M$ RA embryos show abnormal pectoral fin development (arrows, G), and have severe malformations in the forebrain (fb, G), and an expanded visceral cavity (bracket, G). At $10^{-4}\,M$ RA exposure, embryos consist only of a thin trunk (tr, H). Anterior is to the top. Scale bar = 200 μm.

greater than 3.5-fold between stages 25 and 29. The telencephalic ventricle (Fig. 2A, tv) of the forebrain has widened, the eyes are pigmented (arrows), and the optic tecta (ot) have enlarged posterior to the eyes. Embryos exposed to low concentrations (10^{-7}–$10^{-10}\,M$) of RA (Fig. 2B–E) are morphologically normal. In contrast, embryos treated with $10^{-6}\,M$ RA have optic cups that are malformed and rotated anteriorly (arrows, Fig. 2F). The head has enlarged only 2.5-fold over stage 25 embryos. The optic tecta are greatly reduced (asterisk), and the hindbrain (hb) region is shifted anteriorly. The visceral cavity is expanding and appears to be proportionately larger than in control embryos (bracket, Fig. 2F). Other defects also occur in embryos (not shown). The otocysts contain smaller otoliths, and they are irregular in shape; the heart tube is attached by a thin strand of cells to the pericardial wall; and blood cells pool on the ventral side of the embryo at the level of the hindbrain and along the length of the tail. The pectoral fins of control embryos develop just posterior to the vitelline veins, whereas the pectoral fins in RA-treated embryos are posterior and lateral to the otocysts and are slightly smaller (arrowhead, Fig. 2F). In all embryos, frequent muscle movements occur, and the small, bilobed

urinary bladder is developing at the base of the trunk where it is attached to the yolk sac.

1×10^{-5} M *RA*. Embryos exposed to $10^{-5}\,M$ RA (Fig. 2G) lack well-defined eyes and are missing large portions of the midbrain. From stage 25 to stage 29, the area of the head increases only 1.3-fold, remaining similar to that of a stage 25 embryo (compare Figs. 2G and 1G). The visceral cavity is abnormally large relative to the size of the head and trunk, and it covers much of the yolk (bracket). The gut, however, appears normal. A small portion of the forebrain may be present (fb), and some embryos may develop lenses and retinal pigment (not shown). Lenses, in some cases, lie freely exposed on the anterior of the head (not shown). The hindbrain (hb) develops just posterior to any retinal tissue, but the otocysts have been deleted. The pectoral fins develop in an extreme anterior position, such that they are almost lateral to any retinal tissue. Furthermore, the fin structure is abnormal, appearing as thin columns of tissue that extend laterally from the trunk (arrowheads, Fig. 2G). The length of the embryonic axis has increased and, in some embryos, the tip of the tail has detached from the yolk where the small, bilobed urinary bladder is developing (not shown). Blood
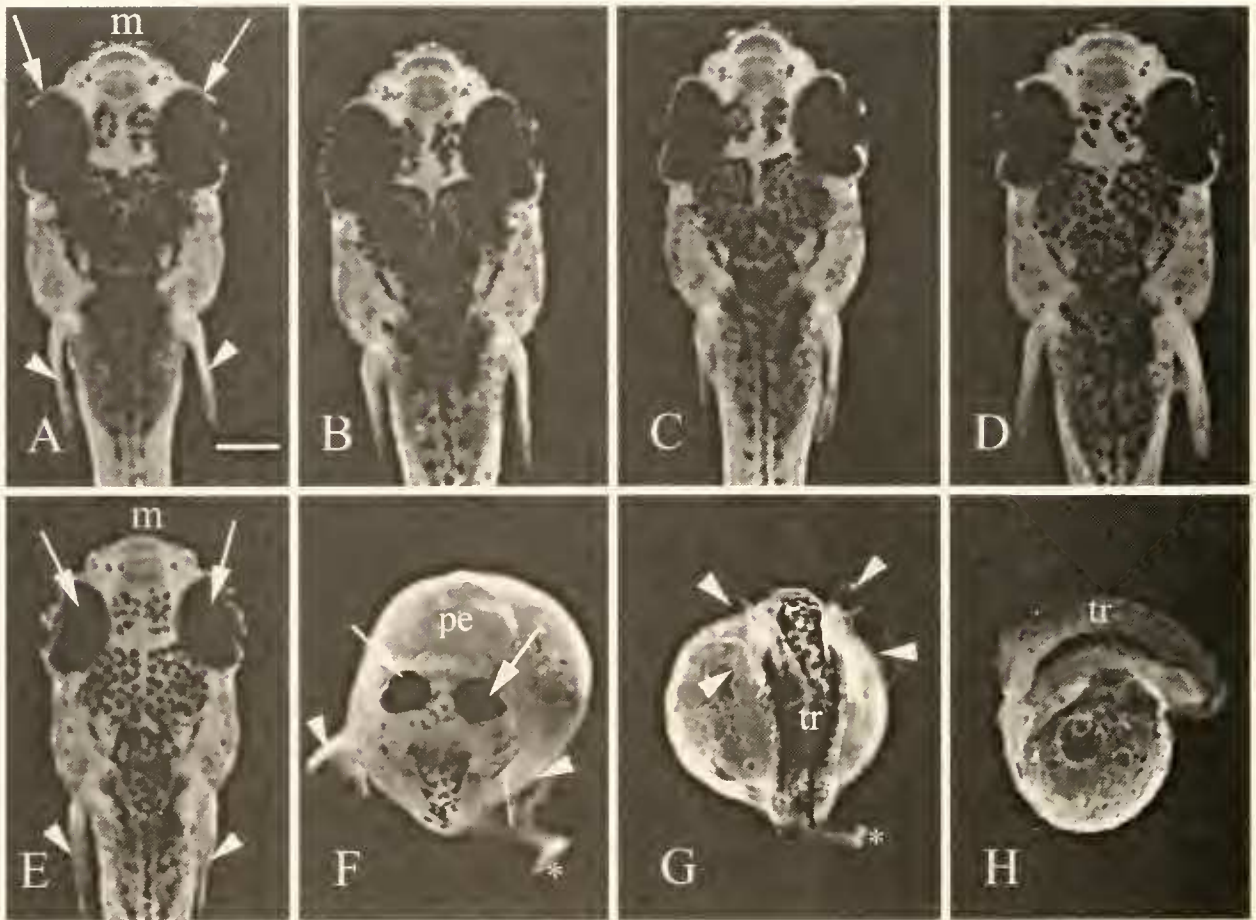
Figure 3. At stage 37, dorsal views of control larvae (A) and larvae exposed at gastrulation to low concentrations of retinoic acid (RA)—10^{-10} M (B), 10^{-9} M (C), 10^{-8} M (D), and 10^{-7} M (E)—show well-developed eyes (arrows, A and E) and pectoral fins (arrowheads, A and E). Larvae exposed at gastrulation to 10^{-6} M RA (F) show anterior and ventral rotation of the eyes (arrows), normal fin development (arrowheads), pericardial edema (pe), and shortened trunks and curled tails (asterisk, F). At 10^{-5} M RA, larvae display multiple pectoral fins (arrowheads, G), a heavily pigmented trunk (tr), and curled tail (asterisk, G). A lateral view of a larva treated at 10^{-4} M RA (H) shows a shortened trunk (tr) atop the yolk. Anterior is to the top (A–G) and to the left (H). Scale bar = 200 μm.

cells are pooled around the urinary bladder, and muscular contractions occur in the trunk, but not as frequently as in the control embryos.

1 × 10^{-4} M RA. Embryos exposed to 10^{-4} M RA (Fig. 2H) lack obvious head structures and appear only as a thin trunk (tr) set on an expanded visceral cavity and gut. Pectoral fins are absent. The urinary bladder is surrounded by blood cells at the base of the trunk where the bladder meets the yolk sac (not shown). Muscular movements occur in some embryos, and a small, stubby tail projects from the trunk (not shown).

Stage 37: Multiple fin phenotypes

1 × 10^{-6} M RA. At stage 37, controls and larvae that have been exposed as gastrulae to 10^{-10} to 10^{-7} M RA are normal in appearance (Fig. 3A–E) and can be induced

to hatch at 10 days post-fertilization. Embryos exposed to greater concentrations of RA do not hatch but survive for an extended period. These larvae are smaller and retain a large volume of yolk (compare Fig. 3A–E with 3F–H). Embryos exposed to 10^{-6} M RA develop into larvae with smaller than normal eyes that display more ventral and anterior rotation than the controls (arrows, Fig. 3F). The pectoral fins, however, approximate normal size (arrowheads, compare Fig. 3A and F) and exhibit a high rate of motor activity. Control larvae and larvae of embryos treated with low concentrations of RA (10^{-10}–10^{-7} M) possess a functional mouth (m, Fig. 3A and E) and jaw, and exhibit rapid opercular movements. The mouths of larvae treated with 10^{-6} M RA as embryos are small and are tucked underneath the forebrain and against the yolk or a large pericardial edema; it is unclear whether

the mouths are functional. The tails are short and curled, and do not exhibit fin development (asterisk, Fig. 3F). Not shown in Figure 3F, the otocysts are irregular in size and shape and are just posterior to the eyes. This is probably due to the midbrain-hindbrain deletion, which causes an anterior shift of the otocysts. The visceral cavity has expanded laterally, and internal organs have developed. The heart, usually located ventrally at the level of the operculum, is contractile but smaller and lies anterior to the gut in a large, balloon-like pericardial edema (pe, Fig. 3F).

1 × 10⁻⁵ M. Exposure to 10^{-5} *M* RA at gastrulation results in larvae that lack most of the forebrain, midbrain, and hindbrain (Fig. 3G). The most prominent feature of these larvae is the development of multiple pectoral fins (arrowheads, Fig. 3G). The supernumerary fins often show a variation in phenotype. Some larvae have two to three pairs of well-developed fins that are often overlapping and move independently of one another (arrowheads, Fig. 3G). Other larvae have more extreme fin phenotypes: *i.e.*, small stubby fins that are fused by soft tissue at the base of the pectoral girdle. Detailed analysis of the multiple-fin phenotype has been described elsewhere (Vandersea *et al.*, in press). The body axis is shortened and the trunk is wide (tr, Fig. 3G); some larvae possess a small, curled tail (asterisk, Fig. 3G) but no ventral, dorsal, or caudal fins. Lenses often lie freely exposed in the anterior head region of the larvae (not shown). The visceral cavities and gut are greatly expanded over the yolk sac. These larvae live for as long as 22 days postfertilization.

1 × 10⁻⁴ M *RA*. Larvae exposed to 10^{-4} *M* RA (Fig. 3H) are very susceptible to bacterial or fungal infections, and about 50% die between stages 29 and 37; but others live for as long as 15 days. In these larvae the tail, pectoral fins, and all of the anterior head structures are absent. A larva viewed laterally (Fig. 3H), rather than dorsally, shows that the trunk (tr) is largely intact. The gut and other internal organs have formed in the visceral cavity, and some larvae possess the remains of a tail, which protrudes as a small stump from the trunk (not shown). The trunk exhibits muscular movements.

Stage 39: Craniofacial and pectoral fin cartilage defects

To determine the effects, at gastrulation, of increasing concentrations of RA on cartilage patterning in the head and fins, larvae were stained with alcian blue at stage 39 (Fig. 4). Camera lucida drawings of the stained larvae were used to aid in the analysis of cranial cartilage and pectoral girdles. For clarity of presentation, we have depicted the elements that make up the braincase as the neurocranial cartilage (Fig. 4E–H), whereas those ele-

ments derived from the seven pharyngeal arches (the mandibular, hyoid, and five branchial arches) and from the pectoral girdle are presented as the pharyngeal-pectoral cartilage (Fig. 4I–L). The identification of cartilage elements was based on comparative descriptions of skull development (de Beer, 1937) and on skull development in medaka (Langille and Hall, 1987) and zebrafish (Cubbage and Mabee, 1996; Schilling and Kimmel, 1997). Abbreviations used in labeling the cartilaginous elements in Figure 4 are listed in Table II (abv). Alcian blue staining of larvae treated during gastrulation with increasing concentrations of RA reveals an overall reduction in the development of cartilage in the head (compare Fig. 4A–D) consistent with the descriptions of the anatomical effects of RA at the earlier stages described above.

At stage 39 in the normal neurocranium (Fig. 4E), the ethmoid plate (ep) joins the lamina orbitonasalis (lo) and trabeculae (t). The epiphyseal bar (eb) joins both the anterior and posterior orbital cartilage (ao, po). Posteriorly, the parachordals (pc) form the base of the neurocranium and fuse with the hypophyseal plate (hp) joining the polar cartilage (pl) with the auditory capsules (ac). Embryos exposed to 5×10^{-7} *M* RA develop (as larvae) a neurocranium that contains all the normal cartilage elements, but is reduced in size (compare Fig. 4E and F). In some cases, the hypophyseal and polar cartilage are slightly malformed (hp and pl, Fig. 4F). Embryos exposed to 10^{-6} *M* RA develop a neurocranium that lacks an epiphyseal bar, as well as anterior and posterior orbital cartilage (Fig. 4G). Notice that the lamina orbitonasalis and trabeculae are only slightly smaller than normal, and the ethmoid plate is present. Furthermore, these elements develop in a more ventral position, close to the level of the pharyngeal skeleton. The posterior neurocranium develops similarly in size and organization in embryos exposed to either 5×10^{-7} *M* RA or 10^{-6} *M* RA (compare Fig. 4F and G). Embryos treated with 10^{-5} *M* RA develop only one neurocranial element—the parachordals (pc, Fig. 4H), which form the posterior base of the neurocranium at the anterior end of the notochord (nc, Fig. 4D).

The pharyngeal-pectoral cartilage at stage 39 (Fig. 4I) consists anteriorly of Meckel's cartilage (mc) which articulates with the pterygoid (p), the quadrate (q), and the hyosymplectic (hs) to form the jaw. In the gill region, the basihyal (bh) and ceratohyals (ch) lie anterior to the centrally located basibranchials (bb) and the three pairs of hypobranchials (hb). Within the branchial arches, five pairs of ceratobranchials (cb) lie ventrally to four paired epibranchials and the pharyngobranchials (not shown). The coracoscapulae (cs) and the proximal radials (pr) compose the pectoral girdle.

Larvae of embryos treated with 5×10^{-7} *M* (Fig. 4J) and 10^{-6} *M* RA (Fig. 4K) do not develop the major cartilage components of the jaw. Although small cartilaginous
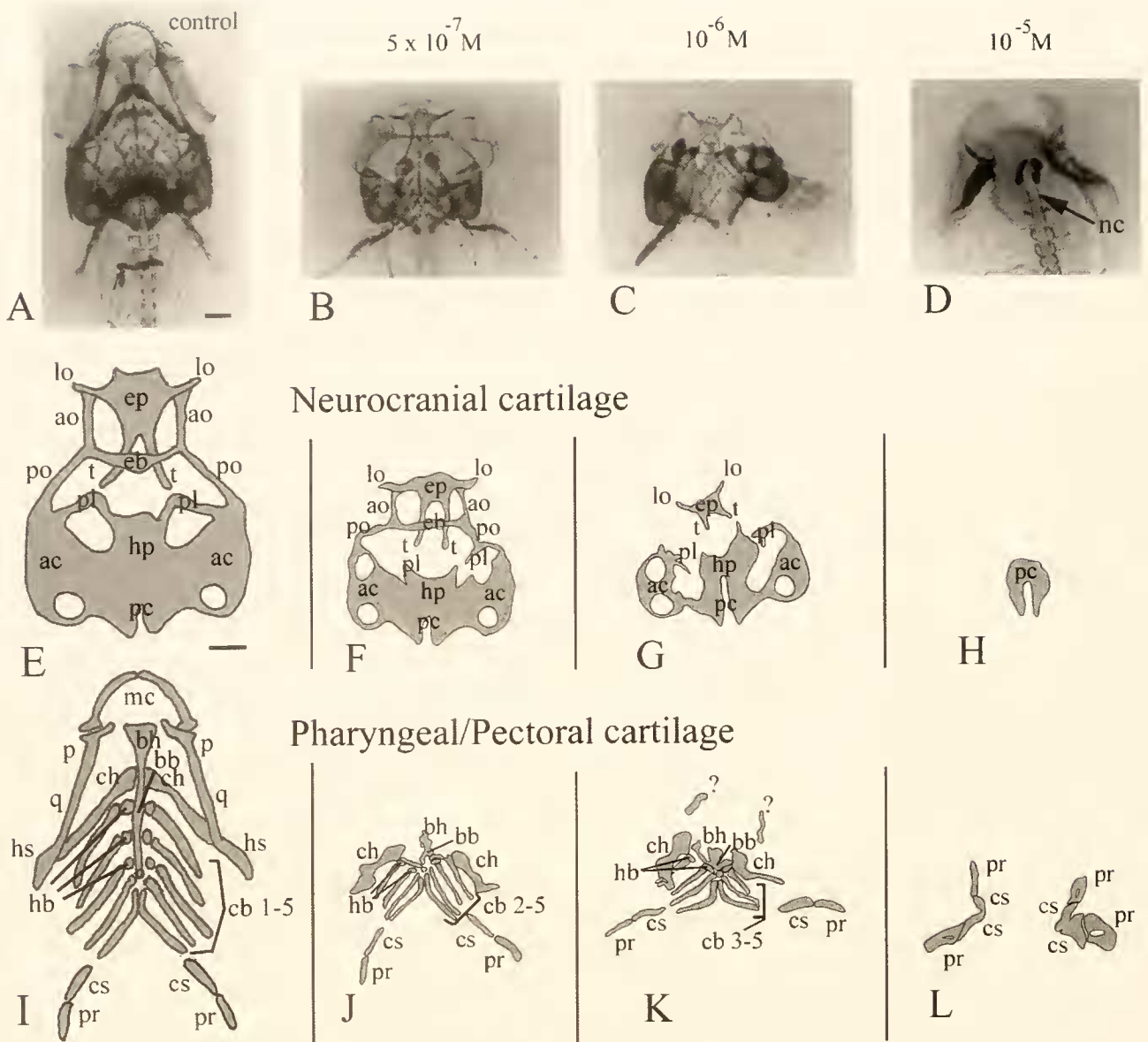
Figure 4. Light micrographs of alcian blue staining (A–D) and camera lucida drawings (E–L) of cartilage elements at stage 39. The figure shows the cartilage elements of control larvae (A, E, and I) and larvae of embryos exposed to retinoic acid (RA) at $5 \times 10^{-7} M$ (B, F, and J), $10^{-6} M$ (C, G, and K), and $10^{-5} M$ (D, H, and L). Camera lucida drawings, which depict a dorsal view of the neurocranial cartilage (E–H) and a ventral view of pharyngeal/pectoral cartilage (I–L), show a progressive loss and malformation of cartilage to increasing concentrations of RA. Abbreviations for cartilage elements are listed in Table II, nc = notochord. Anterior is to the top. Scale bar (A) = 200 μm (A–D) and (E) = 200 μm (E–L).

elements that could represent Meckel's cartilage (question marks, Fig. 4K) are often present, the morphological characteristics of these elements are incomplete, so positive identification is difficult. The basihyal, ceratohyals, and basibranchials are present but shorter and thicker (Fig. 4J and K); moreover, the number of ceratobranchials and hypobranchials that develop may vary. In less extreme cases anterior ceratobranchials are deleted (Fig. 4J and K),

but the posterior elements develop. In the most extreme phenotypes, the ceratobranchials and hypobranchials do not form. The order of the ceratobranchials is distinguished by their associations with the hypobranchials, their position relative to the pectoral girdle cartilage (which develops normally), and the presence of pharyngeal teeth on the fifth ceratobranchial. At both concentrations of RA the epibranchials and pharyngobranchials are

Table II

Analysis of retinoic acid effects on cartilage formation in the head and pectoral girdle

Origin		Skeletal element	Abv[1]	Concentration of retinoic acid			
				$5 \times 10^{-7}\ M$	$10^{-6}\ M$	$10^{-5}\ M$	$10^{-4}\ M$
Neural[2] Crest	Mandibular Arch	Quadrate	(q)	A	A	A	A
		Pterygoid	(p)	A	A	A	A
		Meckel's	(mc)	M/A	M/A	(?)	A
	Hyoid Arch	Hyosymplectic	(hs)	A	A	A	A
		Basihyal	(bh)	M	M	A	A
		Ceratohyals	(ch)	M	M	(?)	A
	Branchial Arches	Epibranchials	—	A	A	A	A
		Pharyngobranchials	—	A	A	A	A
		Basibranchials	(bb)	RN	RN	A	A
		Hypobranchials	(hb)	RN	RN	A	A
		Ceratobranchials	(cb)	RN	RN	A	A
	Neurocranium	Ethmoid plate	(ep)	P	P	(?)	A
		Lamina orbitonasalis	(lo)	P	P	A	A
		Trabeculae	(t)	P	M	(?)	A
		Epiphyseal bar	(eb)	P	A	A	A
		Anterior orbital	(ao)	P	A	A	A
		Posterior orbital	(po)	P	A	A	A
Non-Neural[2] Crest		Polar cartilage	(pl)	P	P	A	A
		Hypophyseal plate	(hp)	P	P	A	A
		Auditory capsule	(ac)	P	M	A	A
		Parachordals	(pc)	P	P	P	A
	Pectoral Girdle	Coracoscapulae	(cs)	P	P	D	A
		Proximal radials	(pr)	P	P	D	A

[1] Abbreviations used in Figure 4.

[2] Based on Langille and Hall, 1988; Schilling and Kimmel, 1997.

Key: P = Present and normal; M = Malformed; RN = Reduced in number; A = Absent; D = Duplicated; ? = Unidentified cartilage.

absent (not shown). Most larvae of embryos exposed to $10^{-5}\ M$ RA lack pharyngeal cartilage, but 94% of these larvae possess multiple fins with two or more pairs of coracoscapulae and proximal radials (Fig. 4L, and Vandersea *et al.*, in press).

Table II lists the cartilaginous skeletal elements that are present in control larvae and in larvae that were exposed, as gastrulating embryos, to increasing concentrations of RA. To aid in the analysis of RA-induced defects, skeletal elements have been grouped according to their embryological origin and their position within the neurocranium or the pharyngeal skeleton. The presence (P) or absence (A) of individual elements is noted, as well as whether the cartilages are malformed (M) or reduced in number (RN). Duplications (D) and unidentified cartilage (?) are also indicated. Elements of the neurocranium are listed in order of their position along the axis, with the anteriormost element, the ethmoid plate, listed first and the posterior elements, the parachordals, listed last. RA causes concentration-dependent deletions of central neurocranial elements at the lowest concentrations of RA and the deletion of more anterior and posterior elements at higher concentrations of RA.

Table II also shows a distinct pattern of deletions in the pharyngeal skeleton which appears to comprise an iterated, segmental set of homologous arches (Romer and Parsons, 1977; Schilling and Kimmel, 1997). In the branchial or gill arches, the epibranchials and pharyngobranchials are the dorsal elements, and the ceratobranchials are the ventral elements. In the mandibular arch the quadrate and pterygoid are considered to be the dorsal homologs, while Meckel's cartilage is believed to correspond to the ventral homolog. The hyosymplectic and ceratohyal cartilages are believed to correspond to the dorsal and ventral homologs, respectively, in the hyoid arch. Notice that dorsal elements in all pharyngeal arches are deleted at lower concentrations of RA than more ventral elements.
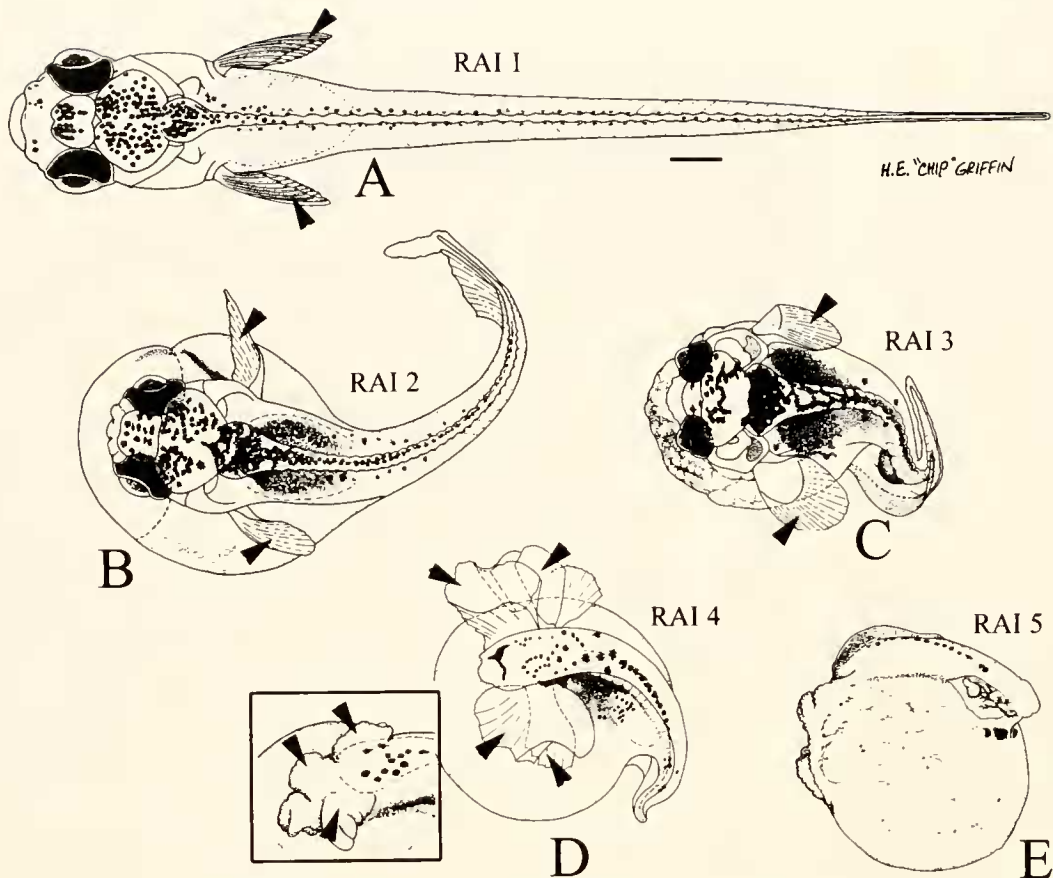
Figure 5. Illustrations of live larvae corresponding to the five retinoic acid (RA) index levels (RAI 1–5). Stage 37 larvae are representative of RAI 1 (A), and larvae with increasing severity of defects due to RA exposure at gastrulation are shown for RAI 2 (B), RAI 3 (C), RAI 4 (D), and RAI 5 (E). Inset (D) shows the variation of duplicated pectoral fins of RAI 4. Arrowheads denote pectoral fins. Dorsal views are shown in A–D and a lateral view in E. Anterior is to the left. Scale bar (A) = 400 μm.

An index of retinoic acid defects

Larvae of *F. heteroclitus* that were exposed at gastrulation to a range of RA concentrations exhibit five distinct phenotypes. We have incorporated these phenotypes into an index of RA defects (RAI). Larvae representative of each level of the index are illustrated in Figure 5 and described (on the basis of morphological observations and alcian blue staining of cartilage) in Table III.

Briefly, RAI 1 represents larvae that are morphologically normal and contain all head and pectoral fin cartilage (Fig. 5A and Table III). RAI 2 larvae show partial deletions of the midbrain-hindbrain border region, with slightly curved tails, normal pectoral fins, and deletions of the cartilage that form in the jaw and anterior gill arches (Fig. 5B and Table III). RAI 3 larvae show additional deletions of structures in the forebrain and midbrain-hindbrain border region, severe truncation of the axis, expansion of the visceral cavity, a thin tubular heart,

and malformations of the cartilages of the neurocranium and anterior gill arches (Fig. 5C and Table III). The most obvious characteristic of RAI 4 larvae is the development of multiple fins, which can range from fully independent pairs of pectoral fins (arrowheads, Fig. 5D) to stubby, malformed pairs of fins (arrowheads, Fig. 5D, inset). RAI 4 larvae also lack forebrain and midbrain-hindbrain border structures and most of the craniofacial cartilage. RAI 5 larvae consist of a muscular trunk with a well-formed gut, but no cartilaginous elements (Fig. 5E and Table III).

To determine whether the phenotypes reflected in the RAI are dependent on the concentration of RA to which the embryos are exposed, we scored 1452 embryos from seven RA experiments and compared the RAI with the level of RA exposure (Fig. 6). Between 97% and 98% of control embryos, DMSO-treated embryos, and embryos exposed to 10^{-7} M RA have an RAI of 1 (Fig. 6, RAI 1). Figure 6 also shows that each exposure concentration between 5×10^{-7} and 10^{-4} M RA exhibits a dominant

Table III

Retinoic acid index

Index level	Description[1]
RAI 1	Larvae appear normal; craniofacial cartilage identical to untreated control embryos.
RAI 2	Partial deletions and distortions of midbrain/hindbrain border region (MB/HB); eyes slightly closer together; axis slightly truncated; heart smaller with pericardial edema, otocysts slightly closer to MB/HB; tail slightly curled; deletions of the quadrate, pterygoid, and hyosymplectic cartilage; malformations of Meckel's cartilage, ceratohyals and the basihyal.
RAI 3	Partial deletion of forebrain (FB); broad deletion of MB/HB border region; eyes smaller, closer together, and ventrally and anteriorly rotated; otocysts shifted anterior; axis severely truncated; curled tail; visceral cavity expanded; thin tube heart with contractions but no circulation; blood cells pooled posteriorly; deletions of the quadrate, pterygoid, hyosymplectic, orbital, epiphyseal, and basibranchial cartilage; malformations or deletion of Meckel's cartilage; malformation of the ethmoid, ceratohyals, basihyal, auditory capsule, basibranchials, hypobranchials, and ceratobranchials.
RAI 4	Broad deletion of FB, MB/HB; otocysts absent; most retinal pigment deleted; heavy pigment on expanded visceral cavity wall; multiple pectoral fins; axis severely truncated and tail curled; urinary bladder and gut present; heart absent; deletions of most craniofacial cartilage; remnants of Meckel's or the ceratohyals may be present; parachordals present; multiple coracoscapulae and proximal radials present.
RAI 5	Major deletions of head and tail with only trunk remaining; urinary bladder and gut present; blood cells pooled posteriorly; muscular movements of trunk present; no cartilaginous staining present.

[1] Descriptions are summaries of the larval anatomy at stage 37 and cartilage staining at stage 39.

index level that includes most of the embryos exposed to that concentration at gastrulation: $5 \times 10^{-7} M$ RA, 90% of embryos fall into RAI 2; $10^{-6} M$ RA, 88% in RAI 3; $10^{-5} M$ RA, 91% in RAI 4; $10^{-4} M$ RA, 93% in RAI 5. The ability of RA to induce reproducible phenotypes in a large number of embryos makes *F. heteroclitus* an important embryonic model for the understanding of molecular and genetic interactions of the RA signaling pathways.

Discussion

We have described brain, craniofacial, and pectoral fin defects arising from the exposure of *F. heteroclitus* embryos to increasing concentrations of exogenous retinoic acid during gastrulation. RA-treated embryos, like control embryos, gastrulate and form an axis, but by stage 25, they demonstrate dose-dependent differences in axial patterning. Moderate RA exposure during gastrulation leads to axial patterning defects in the tail, heart, midbrain-hindbrain, and the craniofacial cartilage. High concentrations of RA further disrupt the pectoral fins, otocysts, forebrain, and posterior hindbrain structures (including cartilage). However, patterning of the gut and trunk appear normal, even at high RA exposures. We have used RA phenotypes to establish an RA index that shows low inter-experimental variability. The index should be useful in understanding RA signaling pathways.

Cellular events that may contribute to RA-induced phenotypes

Gastrulation and neural induction. Embryos exposed to exogenous RA at 50% epiboly continue to gastrulate and show no immediate signs of cell death or toxic response. The overall patterns of development of treated and control embryos at 25°C are similar prior to stage 25, some 27 hours after RA exposure. Other responses to RA argue against an immediate toxic response: *i.e.*, embryos exposed to the highest RA concentrations live for more than 2 weeks, show normal gut and somatic trunk muscle development, and exhibit frequent muscle contractions.

Although we have not examined in detail the effects of RA on gastrulation, it is possible that the patterning defects we observe stem, in part, from subtle changes in cellular migration patterns during gastrulation. Gastrulation in *F. heteroclitus* occurs by the ingression of superficial deep cells at the margin of the blastoderm during early epiboly (stage $13-13^{1/2}$, 12 hpf at 25°C; Trinkaus, 1996). The detailed studies of Trinkaus and colleagues provide background information on development in this species, and the large size and transparency of the embryo contribute to ease of observation. Together, these factors make *F. heteroclitus* embryos excellent candidates for lineage studies to determine whether RA leads to altered migration patterns of cells during gastrulation.

Exposure to RA may disrupt the interactions that occur between mesoderm and ectoderm during gastrulation—interactions shown by classical embryological and recent molecular studies to be critical for normal neural induction of the brain and spinal cord (Spemann and Mangold, 1924; Tanabe and Jessell, 1996; Elinson and Kao, 1993). It has been shown in *X. laevis*, that treatment with RA during gastrulation affects both mesoderm (Cho and De Robertis, 1990; Sive *et al.*, 1990; Sive and Cheng, 1991;
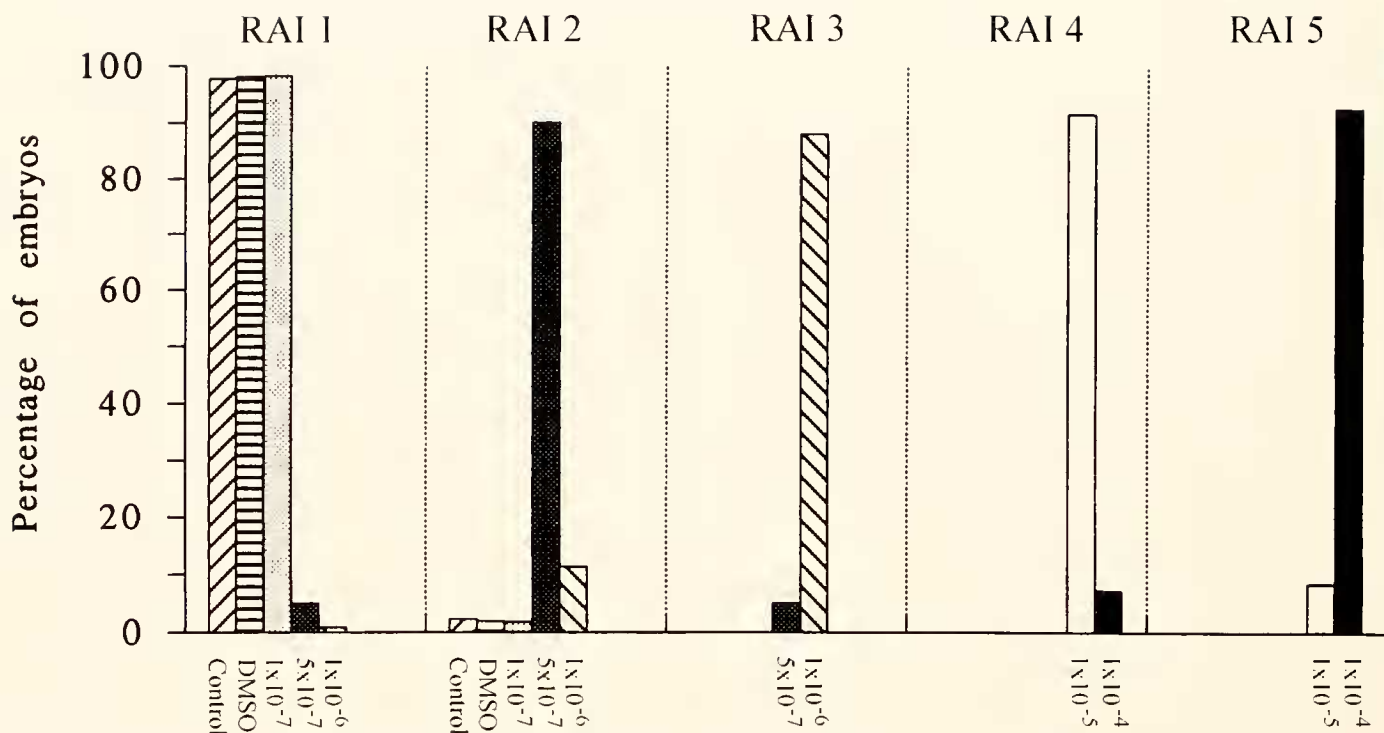
Figure 6. Distributions of embryos categorized by retinoic acid (RA) index level. The graph shows the percentage of control larvae ($n = 205$) and larvae treated at gastrulation with DMSO ($n = 192$) or RA at $10^{-7} M$ ($n = 214$), $5 \times 10^{-7} M$ ($n = 100$), $10^{-6} M$ ($n = 231$), $10^{-5} M$ ($n = 280$), $10^{-4} M$ ($n = 230$) that fall within each RAI level.

Ruiz i Altaba and Jessell, 1991a) and ectoderm (Ruiz i Altaba and Jessell, 1991b). Transplantation experiments, as pioneered in *F. heteroclitus* by Oppenheimer (1936), between RA-treated and control ectoderm and mesoderm may resolve which of these effects on ectoderm or mesoderm is the more relevant to the midbrain-hindbrain deletions and craniofacial defects we observe.

Cell death and cell proliferation. Proper patterning of early development depends on both embryonic growth and programmed cell death. Studies carried out in zebrafish have shown that RA exposure leads to midbrain-hindbrain deletions, demonstrated by the absence of cells expressing the marker protein, engrailed, which is diagnostic for this region (Holder and Hill, 1991). Stainier and Fishman (1992) have suggested, from separate observations of RA-treated zebrafish, that opaque cells found in the affected midbrain-hindbrain region correspond to cells undergoing cell death. We find that *F. heteroclitus* embryos exposed to concentrations of RA greater than $10^{-7} M$ gastrulate and form an axis similar to that of control embryos. However, at stage 25, RA-treated embryos show localized opaque zones in the brain and tail, similar to those described in zebrafish. In subsequent stages, the opaque regions are

cleared from the embryo, and structures are deleted within these regions. Cell death in opaque zones may partially account for the severe truncation of the axis that is evident in older embryos.

A comparison of normal and RA-exposed embryos shows differences that may not be fully explained by localized cell death. At stage 25, control and RA-treated embryos display only slight overall differences in size; by stage 29, however, considerable size differences are obvious. For example, head structures in control embryos have enlarged relative to stage 25 embryos, whereas similar structures in RA-treated embryos have not. Therefore, increased levels of RA may also disrupt signaling events necessary for cellular proliferation in the embryo. Thus, our observations point to two developmental periods at which effects produced by RA exposure during gastrulation lead to changes in embryonic size: (1) between stage 21 and stage 25, cell death may be increased in RA-treated embryos; (2) between stages 25 and 29, cell proliferation may be decreased in RA-exposed embryos. Further investigations in *F. heteroclitus* by TUNEL assays for cell death and BrdU assays for cell proliferation should clarify the effects of RA exposure at gastrulation on later development.

Effects of RA on axial specification and cartilage patterning

RA-treated embryos survive for up to 22 days and show extensive development of cartilaginous skeletal elements. This has permitted a more detailed analysis of RA-induced craniofacial and pectoral fin skeletal defects than has been undertaken for other species. Our results show that the development of many craniofacial and pectoral fin cartilage elements is altered in response to RA exposure during gastrulation. Dose-dependent deletions occur in both neurocranial and pharyngeal skeletal elements, while duplications and deletions are observed for pectoral girdle and fin elements.

In the neurocranium, the orbitals and epiphyseal bar, which are cartilage elements centrally located along the anterior-posterior (A/P) axis, are deleted at lower concentrations of RA than are the ethmoid plate and the parachordals, which are elements at the anterior and posterior extremes. These results suggest that RA has a concentration-dependent effect, either on the developmental regulation of specific neural cranial elements, or on the specification of their ultimate position along the A/P axis. Although patterning of the craniofacial region is generally believed to be conserved in evolution, the origin of the neurocranium—whether from mesoderm or neural crest—is a matter of contention. Extirpation of neural crest cells in medaka embryos results in defects of the craniofacial cartilage (Langille and Hall, 1988), demonstrating the importance of neural crest for normal head development. These studies suggest that the anteriormost elements of the neurocranium, the ethmoid plate and trabeculae, are derived from neural crest cells that migrate from the mesencephalon, whereas the more centrally located elements, orbitals and epiphyseal bar, receive neural crest contributions from both the mesencephalon and the preotic rhombencephalon (Langille and Hall, 1988). Posterior elements of the neurocranium are believed to be derived from mesoderm (Langille and Hall, 1988). However, recent quail-chick transplantation studies suggest that most of the neurocranium is mesoderm-derived (Couly *et al.,* 1993), except for specific neural-crest-derived regions corresponding to sites at which craniofacial muscles attach (Koentges and Lumsden, 1996). The patterns of deletions of cartilaginous elements we observe at moderate RA concentrations seem to be unrelated to their embryological origin—whether that is neural crest or mesoderm. Thus, RA is more likely to be affecting positional information given to cells along the A/P axis.

The pharyngeal skeleton consists of a set of seven segmented arch homologs, each consisting of dorsal and ventral elements that give rise to specific cartilage elements (Romer and Parsons, 1977; Schilling and Kimmel, 1997). We observe two patterns of cartilage deletions in response to increasing concentrations of RA. First, the dorsal cartilage elements in each of the arches are deleted at a lower concentration of RA than the more ventral cartilage elements. For example, in the neurocranial cartilage of larvae exposed to $5 \times 10^{-7} M$ RA as gastrulae, the ventral elements of all seven arches can be found (Meckel's cartilage in the mandibular arch, the ceratohyal in the hyoid arch, and the ceratobranchials in the branchial arches). The more dorsal elements (quadrate and pterygoid in the mandibular arch, hyosymplectic in the hyoid arch, and epibranchials or pharyngobranchials in the branchial arches) are all absent.

The second pattern involves the deletion of ventral elements of each arch and occurs in a noncontiguous fashion with respect to the A/P axis. Larvae treated as gastrulae with $5 \times 10^{-7} M$ RA show deletions of one pair of ceratobrachials, whereas the ceratohyals in the hyoid arch and, in many cases, Meckel's cartilage in the mandibular arch remain. All of these cartilages are ventral elements, with the ceratohyals more centrally located along the A/P axis of the head. Although the order of the deleted ceratobranchials cannot be established definitively, they are not the tooth-bearing fifth pair of ceratobranchials, which are still present. The discontinuity of deleted ventral cartilages, relative to their position along the A/P axis, is seen at higher concentrations of RA where Meckel's cartilage and one or more additional pair of ceratobranchials are eliminated before the ceratohyals. To emphasize this important point, the cartilage derived from the ventral element of the second arch is formed; but the ventral elements of first and third or fourth arches are deleted.

The effects of exogenous RA on embryos have been explained by disruption of endogenous gradients of RA on the early patterning of embryonic tissues (Durston *et al.,* 1989). In vertebrates, RA has been shown to be important in patterning the embryonic axis (Sive *et al.,* 1990; Kessel, 1992; Conlon, 1995). All of the cartilage elements of the pharyngeal skeleton are believed to be derived from neural crest cells that migrate from midbrain and from specific rhombomeres of the hindbrain (Langille and Hall, 1988, 1993; Lumsden *et al.,* 1991; Couly *et al.,* 1993). However, different skeletal elements in the same arch, and even a single cartilage element within an arch, may receive contributions of neural crest cells from more than one specific axial level (Koentges and Lumsden, 1996). Recent studies in zebrafish suggest that dorsal and ventral elements in a given arch originate from separate sites of chondrification within the same condensation of precartilage cells (Schilling and Kimmel, 1997). In the mandibular arch, for example, the quadrate and Meckel's cartilage both arise from a single precartilage condensation, with the quadrate forming before Meckel's cartilage (Schilling and Kimmel, 1997). Our results suggest that the dorsal and ventral cartilage elements of the pharyngeal arches

are differentially sensitive to early exposure to RA and may originate from different populations of neural crest cells along the embryonic axis. Furthermore, the noncontiguous pattern of deletions of ventral elements indicates a more complex regulation or axial organization than previously recognized.

Although most of the RA-induced patterning defects we describe in this study represent deletions of specific structures, exposure of *F. heteroclitus* embryos to 1×10^{-5} *M* RA during gastrulation causes duplications of pectoral fins (described in further detail in Vandersea *et al.*, in press). Parallel studies in zebrafish also show duplicated pectoral fins at defined RA concentrations (Vandersea *et al.*, in press). Lower body and limb duplications have been shown to be induced by RA when administered during pregastrulation stages to mouse embryos (Rutledge *et al.*, 1994). Our results demonstrate that the phenotypic response to RA at gastrulation may be evolutionarily conserved and suggest that RA may be an early signaling molecule for axial specification of vertebrate limbs. The induction of duplications of specific structures is consistent with current ideas that the mechanism by which exogenous RA disrupts developmental patterning is mis-expression of patterning genes, such as Hox and Otx2 genes (Conlon, 1995).

Molecular aspects of RA action—Hox gene involvement

RA is an endogenous regulator of patterning in vertebrate embryos; at the molecular level, RA is believed to exert its patterning influences by the temporal and spatial regulation of Hox and other homeobox-containing genes (Simeone *et al.*, 1990; Papalopulu *et al.*, 1991; Langston and Gudas, 1992; and Studer *et al.*, 1994). In this paper we have shown that brain and skeletal elements of the *F. heteroclitus* head exhibit dose-dependent deletions in response to RA exposure during gastrulation. By supplying excess RA, we are disrupting the natural levels of RA in the embryos; this in turn may alter homeobox and Hox gene expression, resulting in developmental defects (Taira *et al.*, 1994; Conlon, 1995; Hill *et al.*, 1995; Alexandre *et al.*, 1996). Our work provides a model species that permits large numbers of synchronous embryos to be treated with RA at gastrulation. RA-treated *F. heteroclitus* embryos develop with distinct, reproducible phenotypes that may be useful in resolving the molecular details of RA-signaling pathways and the role of Hox gene expression.

RA signaling pathways may be sensitive to disruption by xenobiotics

The craniofacial defects we have characterized in this study of *F. heteroclitus* are similar to defects that have been described in fish and other vertebrates exposed to various xenobiotics (Weis and Weis, 1989). RA is critical for normal patterning of the craniofacial region and the heart (Means and Gudas, 1995; Conlon, 1995), and defects induced in these regions by various xenobiotics suggest that they may act by disrupting RA signaling pathways. RA acts by binding to receptors that are members of a large superfamily of steroid and thyroid hormone receptors (Leid *et al.*, 1993). Certain xenobiotics may mimic RA or disrupt the RA signaling pathway by binding or interfering with this class of receptors. For example, the insect growth regulator methoprene is teratogenic in mice (Unsworth *et al.*, 1974) and can activate one class of retinoid receptors in expression assays (Harmon *et al.*, 1995).

In this paper we have established a dose-response index describing the phenotypes resulting from increasing doses of RA. Similar index phenotypes are also identifiable in RA-exposed zebrafish embryos (Vandersea *et al.*, in press; and unpubl. data), suggesting that the mechanism by which RA induces defects is evolutionarily conserved. *F. heteroclitus* and zebrafish are, respectively, estuarine and freshwater fish species that are widely used in toxicology studies. The index we describe should be useful in embryo-based assays for toxicological and environmental monitoring studies by permitting xenobiotic effects to be ranked and quantified in exposed embryos whose defects resemble those resulting from RA exposure. This index should also aid in defining the mechanisms by which xenobiotics act and the concentrations that can be tolerated in the environment.

Literature Cited

Akimenko, M. A., and M. Ekker. 1995. Anterior duplication of the sonic hedgehog expression pattern in the pectoral fin buds of zebrafish treated with retinoic acid. *Dev. Biol.* **170:** 243–247.

Alexandre, D., J. D. W. Clarke, E. Oxtoby, Y-L. Yan, T. Jowett, and N. Holder. 1996. Ectopic expression of *Hoxa-1* in the zebrafish alters the fate of the mandibular arch neural crest and phenocopies a retinoic acid-induced phenotype. *Development* **122:** 735–746.

Armstrong, P. B., and J. S. Child. 1965. Stages in the normal development of *Fundulus heteroclitus. Biol. Bull.* **123:** 143–168.

Chen, Y., L. Huang, A. F. Russo, and M. Solursh. 1992. Retinoic acid is enriched in Hensen's node and is developmentally regulated in the early chick embryo. *Proc. Natl. Acad. Sci. USA* **89:** 10056–10059.

Chen, Y., L. Huang, and M. Solursh. 1994. A concentration of retinoids in the early *Xenopus laevis* embryo. *Dev. Biol.* **161:** 70–76.

Cho, K. W. Y., and E. M. De Robertis. 1990. Differential activation of *Xenopus* homeobox genes by mesoderm-inducing growth factors and retinoic acid. *Genes Dev.* **4:** 1910–1916.

Conlon, R. A. 1995. Retinoic acid and pattern formation in vertebrates. *Trends Genet.* **11:** 314–319.

Couly, G. F., P. M. Coltey, and N. M. Le Douarin. 1993. The triple origin of skull in higher vertebrates: a study in quail-chick chimeras. *Development* **117:** 409–429.

Cubbage, C. C., and P. M. Mabee. 1996. Development of the cranium and paired fins in the zebrafish *Danio rerio* (Ostariophysi, Cyprinidae). *J. Morphol.* **229:** 1–40.

de Beer, G. R. 1937. *The Development of the Vertebrate Skull.* Oxford University Press, Oxford, UK. Reprinted 1985. Chicago University Press, Chicago, IL.

Dingerkus, G., and D. L. Uhler. 1977. Enzyme clearing of Alcian Blue stained whole small vertebrates for demonstration of cartilage. *Stain Technol.* **52:** 229–231.

Durston, A. J., J. P. M. Timmermans, W. J. Hage, H. F. J. Hendriks, N. J. de Vries, M. Heideveld, and P. D. Nieuwkoop. 1989. Retinoic acid causes an anteroposterior transformation in the developing central nervous system. *Nature* **340:** 140–144.

Elinson, R. P., and K. R. Kao. 1993. Axis specification and head induction in vertebrate embryos. Pp. 1–41 in *The Skull,* J. Hanken and B. K. Hall, eds. University of Chicago Press, Chicago, IL.

Gale, E., V. Prince, A. Lumsden, J. Clarke, N. Holder, and M. Maden. 1996. Late effects of retinoic acid on neural crest and aspects of rhombomere identity. *Development* **122:** 783–793.

Grunwald, D. J., C. B. Kimmel, M. Westerfield, C. Walker, and G. Streisinger. 1988. A neural degeneration mutation that spares primary neurons in the zebrafish. *Dev. Biol.* **126:** 115–125.

Harmon, M. A., M. F. Boehm, R. A. Heyman, and D. J. Mangelsdorf. 1995. Activation of mammalian retinoid X receptors by the insect growth regulator methoprene. *Proc. Natl. Acad. Sci. USA* **92:** 6157–6160.

Hill, J., J. D. W. Clarke, N. Vargesson, T. Jowett, and N. Holder. 1995. Exogenous retinoic acid causes alterations in the development of the hindbrain and midbrain of the zebrafish embryo including positional respecification of the Mauthner neuron. *Mech. Dev.* **50:** 3–16.

Hogan, B., C. Thaller, and G. Eichele. 1992. Evidence that Hensen's node is a site of retinoic acid synthesis. *Nature* **359:** 237–241.

Holder, N., and J. Hill. 1991. Retinoic acid modifies development of the midbrain-hindbrain border and affects cranial ganglion formation in zebrafish embryos. *Development* **113:** 1159–1170.

Hunt, P., M. Gulisano, M. Cook, M. Sham, A. Faiella, D. Wilkinson, E. Boncinelli, and R. Krumlauf. 1991. A distinct Hox code for the branchial region of the head. *Nature* **353:** 861–864.

Kessel, M. 1992. Respecification of vertebral identities by retinoic acid. *Development* **115:** 487–501.

Kessel, M., and P. Gruss. 1991. Homeotic transformations of murine vertebrae and concomitant alteration of Hox codes induced by retinoic acid. *Cell* **67:** 89–104.

Koentges, G., and A. Lumsden. 1996. Rhombencephalic neural crest segmentation is preserved throughout craniofacial ontogeny. *Development* **122:** 3229–3242.

Krumlauf, R. 1994. Hox genes in vertebrate development. *Cell* **78:** 191–201.

Langille, R. M., and B. K. Hall. 1987. Development of the head skeleton of the Japanese medaka, *Oryzias latipes* Teleostei. *J. Morphol.* **193:** 135–158.

Langille, R. M., and B. K. Hall. 1988. Role of the neural crest in development of the cartilaginous cranial and visceral skeleton of the medaka, *Oryzias latipes* Teleostei. *Anat. Embryol.* **177:** 297–305.

Langille, R. M., and B. K. Hall. 1993. Pattern formation and the neural crest. Pp. 77–111 in *The Skull,* J. Hanken and B. K. Hall, eds. University of Chicago Press, Chicago, IL.

Langston, A. W., and L. J. Gudas. 1992. Identification of a retinoic acid responsive enhancer 3' of the murine homeobox gene *Hox 1.6. Mech. Dev.* **38:** 217–228.

Leid, M., P. Kastner, B. Durand, A. Krust, P. Leroy, R. Lyons, C. Mendelsohn, S. Nagpal, H. Nakshatri, C. Reibel, M. Saunders, and P. Chambon. 1993. Retinoic acid signal transduction pathways. *Annals N.Y. Acad. Sci.* **684:** 19–34.

Leonard, L., C. Horton, M. Maden, and J. A. Pizzey. 1995. Anteriorization of CRABP-I expression by retinoic acid in the developing mouse central nervous system in its relationship to teratogenesis. *Dev. Biol.* **168:** 514–528.

Lohnes, D., M. Mark, C. Mendelsohn, P. Dolle, D. Decimo, M. LeMeur, A. Dierich, P. Gorry, and P. Chambon. 1995. Developmental roles of the retinoic acid receptors. *J. Steroid Biochem. Mol. Biol.* **53:** 475–486.

Lumsden, A., N. Spawson, and A. Graham. 1991. Segmental origin and migration of neural crest cells in the hindbrain region of the chick embryo. *Development* **8:** 329–335.

Marshall, H., S. Nonchev, M. H. Sham, I. Muchamore, A. Lumsden, and R. Krumlauf. 1992. Retinoic acid alters hindbrain Hox code and induces transformation of rhombomeres 2/3 into a 4/5 identity. *Nature* **360:** 737–741.

Marshall, H., M. Studer, H. Popperl, S. Aparicio, A. Kuroiwa, S. Brenner, and R. Krumlauf. 1994. A conserved retinoic acid response element required for early expression of the homeobox gene *Hox b-1. Nature* **370:** 567–571.

Means, A. L., and L. J. Gudas. 1995. The roles of retinoids in vertebrate development. *Annu. Rev. Biochem.* **64:** 201–233.

Minucci, S., J. P. Saint-Jeannet, R. Toyama, G. Scita, L. M. DeLuca, M. Tiara, A. A. Levin, K. Ozato, and I. B. Dawid. 1996. Retinoid X receptor-selective ligands produce malformations in *Xenopus* embryos. *Proc. Natl. Acad. Sci. USA* **93:** 1803–1807.

Noden, D. M. 1975. An analysis of the migratory behavior of avian cephalic neural crest cells. *Dev. Biol.* **42:** 106–130.

Oppenheimer, J. 1936. Transplantation experiments on developing teleosts (*Fundulus* and *Perca*). *J. Exp. Zool.* **72:** 409–437.

Oppenheimer, J. 1937. The normal stages of *Fundulus heteroclitus. Anat. Rec.* **68:** 1–15.

Papalopulu, N., R. Lovell-Badge, and R. Krumlauf. 1991. The expression of murine *Hox-2* genes is dependent on the differentiation pathway and displays a collinear sensitivity to retinoic acid in F9 cells and *Xenopus* embryos. *Nucleic Acids Res.* **19:** 5497–5506.

Romer, A. S., and T. S. Parsons. 1977. *The Vertebrate Body.* Saunders College Publishing, Philadelphia.

Ruiz i Altaba, A., and T. M. Jessell. 1991a. Retinoic acid modifies mesodermal patterning in early *Xenopus* embryos. *Genes Dev.* **5:** 175–187.

Ruiz i Altaba, A., and T. M. Jessell. 1991b. Retinoic acid modifies the pattern of cell differentiation in the central nervous system of neurula stage *Xenopus* embryos. *Development* **112:** 945–958.

Rutledge, J. C., A. G. Shourbaji, L. A. Hughes, J. E. Polifka, Y. P. Cruz, J. B. Bishop, and W. M. Generoso. 1994. Limb and lower-

body duplications induced by retinoic acid in mice. *Proc. Natl. Acad. Sci. USA* **91**: 5436–5440.

Schilling, T. F., and C. B. Kimmel. 1994. Segment and cell type lineage restrictions during pharyngeal arch development in the zebrafish embryo. *Development* **120**: 483–494.

Schilling, T. F., and C. B. Kimmel. 1997. Musculoskeletal patterning in the pharyngeal segments of the zebrafish embryo. *Development* **124**: 2945–2960.

Schuh, T. J., B. L. Hall, J. C. Kraft, M. L. Privalsky, and D. Kimelman. 1993. v-erb A and citral reduce the teratogenic effects of all-trans retinoic acid and retinol, respectively, in *Xenopus* embryos. *Development* **119**: 785–795.

Sharp, J. R., and J. M. Neff. 1980. Effects of the duration of exposure to mercuric chloride on the embryogenesis of the estuarine teleost, *Fundulus heteroclitus. Mar. Environ. Res.* **3**: 195–203.

Sharp, J. R., and J. M. Neff. 1985. Age-dependent response differences of *Fundulus heteroclitus* embryos following chronic exposure to mercury. P. 281 in *Marine Pollution and Physiology: Recent Advances,* P. J. Vernberg, F. P. Thurberg, A. Calabrese, and W. B. Vernberg, eds. University of South Carolina Press, Columbia, SC.

Simeone, A., D. Acampora, L. Arcioni, P. W. Andrews, E. Boncinelli, and F. Mavilio. 1990. Sequential activation of HOX2 homeobox genes by retinoic acid in human embryonal carcinoma cells. *Nature* **346**: 763–766.

Sive, H. L., and P. F. Cheng. 1991. Retinoic acid perturbs the expression of *Xhox.lab* genes and alters mesodermal determination in *Xenopus laevis. Genes Dev.* **5**: 1321–1332.

Sive, H. L., B. W. Draper, R. M. Harland, and H. Weintraub. 1990. Identification of a retinoic acid-sensitive period during primary axis formation in *Xenopus laevis. Genes Dev.* **4**: 932–942.

Solberg, A. N. 1938. The development of a bony fish. Pp. 378–379 in *Experimental Embryology Techniques and Procedures,* R. Rugh, ed. Burgess Publishing Co. Minneapolis, MN.

Spemann, H., and H. Mangold. 1924. Induction of embryonic primordia by implantation of organizers from a different species. Pp. 144–184 in *Foundations of Experimental Embryology,* B. H. Willier and J. M. Oppenheimer, eds. Hafner, New York.

Stainier, D. Y. R., and M. C. Fishman. 1992. Patterning the zebrafish heart tube: acquisition of anteroposterior polarity. *Dev. Biol.* **153**: 91–101.

Studer, M., H. Popperl, H. Marshall, A. Kuroiwa, and R. Krumlauf. 1994. Role of a conserved retinoic acid response element in rhombomere restriction of *Hox b-1. Science* **265**: 1729–1732.

Tabin, C. 1995. The initiation of the limb bud: growth factors, Hox genes and retinoids. *Cell* **80**: 671–674.

Taira, M., M. Jamrich, P. J. Good, and I. B. Dawid. 1994. The LIM domain-containing homeobox gene XLIM-1 is expressed specifically in the organizer region of *Xenopus* gastrula embryos. *Genes Dev.* **6**: 356–366.

Tanabe, Y., and T. M. Jessell. 1996. Diversity and pattern in the developing spinal cord. *Science* **274**: 1115–1122.

Tickle, C. 1995. Vertebrate limb development. *Curr. Opin. Genet. Dev.* **5**: 478–484.

Trinkaus, J. P. 1996. Ingression during early gastrulation of *Fundulus. Dev. Biol.* **177**: 356–370.

Unsworth, B., S. Hennen, and A. Krishnakumaran. 1974. Teratogenic evaluation of terpenoid derivatives. *Life Sci.* **15**: 1649–1655.

Vandersea, M. W., P. Fleming, R. A. McCarthy, and D. Smith. 1998. Fin duplications and deletions induced by disruption of retinoic acid signaling. *Dev. Genes Evol.* (in press).

Weis, P., and J. S. Weis. 1977. Methylmercury teratogenesis in the killifish, *Fundulus heteroclitus. Teratology* **16**: 317–326.

Weis, J. S., and P. Weis. 1989. Effects of environmental pollutants on early fish development. *Rev. Aquat. Sci.* **1**: 45–73.

Wood, H., G. Pall, and G. Morriss-Kay. 1994. Exposure to retinoic acid before or after the onset of somitogenesis reveals separate effects on rhombomeric segmentation and 3' *HoxB* gene expression domains. *Development* **120**: 2279–2285.

Zilliacus, J., A. P. H. Wright, J. Carlstedt-Duke, and J. Gustafsson. 1995. Structural determinants of DNA-binding specificity by steroid receptors. *Mol. Endocrinol.* **9**: 389–399.